DOI: http://dx.doi.org/10.7551/978-0-262-31709-2-ch151

From Microbiology to Microcontrollers:
Robot Search Patterns Inspired by T Cell Movement

G. Matthew Fricke[1], François Asperti-Boursin[2], Joshua P. Hecker[1], Judy L. Cannon[2,3] and Melanie E. Moses[1,4,5]
[1]Department of Computer Science, [2]Department of Molecular Genetics and Microbiology, [3]Department of Pathology,
[4]Department of Biology, University of New Mexico, Albuquerque, NM 87131
[5]Santa Fe Institute, Santa Fe, New Mexico 87501
mfricke@cs.unm.edu

Abstract

In order to trigger an adaptive immune response, T cells move through lymph nodes searching for dendritic cells that carry antigens indicative of infection. We observe T cell movement in lymph nodes and implement those movement patterns as a search strategy in a team of simulated robots. We find that the distribution of step-sizes taken by T cells are best described by heavy-tailed (Lévy-like) distributions. Such distributions are characterized by many small steps and rare large steps. Our simulations show that heavy-tailed motion leads to dramatically faster search compared to Brownian motion, both in groups of T cells and in teams of robots. The mechanisms that cause heavy-tailed movement patterns in T cells are not fully understood. However, in robot simulations we find that heavy-tailed movement improves search speed whether that movement is caused by rules intrinsic to the robots or by adaptive response to extrinsic factors in the environment.

Introduction

Biologically-inspired computation has a long history. Neural networks, genetic algorithms, and cellular automata are just a few well-known examples. In this study we observe immune cells searching within the three-dimensional space of mouse lymph nodes. We characterize T cell movement, demonstrate its effectiveness as a search strategy, and implement a similar search in simulated robots foraging for resources.

Robot teams can be used to perform real-world tasks such as surveying planetary surfaces and interplanetary space (Fink et al., 2005), land and sea mine clearance (Weber, 1995), pollution mapping by subsurface robots (Hu et al., 2011), and survivor location in hazardous environments (Birk and Carpin, 2006). The success of robot teams searching for resources in an unknown environment depends on the efficiency of the random search strategy employed.

Biological Context

In order to mount an effective immune response, T cells must be activated in lymph nodes (Fig. 1). Activation occurs when a T cell discovers and interacts with a dendritic cell (DC) presenting a specific antigen. Antigens are markers that identify particular pathogens. Each T cell matches a particular range of antigens. A DC presenting an antigen indicates that the corresponding pathogen has been encountered in the organism's tissues. If a T cell encounters a DC displaying cognate antigen then an immune response is triggered (Mackay et al., 2000).

To facilitate T cell activation, T cells and DCs interact within the T cell zone of lymph nodes (Fig. 1). The T cell zone is on the order of $1\,\mathrm{mm}^3$ in the inguinal mouse lymph nodes we analyse. T cells and DCs are on the order of $10\,\mu\mathrm{m}$ in diameter, so for each lymph node the T cell searches a space some 10^8 times its own volume. In secondary lymphoid organs, DCs usually comprise between 1% and 5% of the T cell zone's total cell population. Each T cell interacts with as many DCs as possible in order to maximize the probability of detecting a matching antigen (Mirsky et al., 2011). This imposes the need for efficient random search to mount an immune response.

Early response to infection depends on the rate at which DCs are discovered by T cells in the lymph node. The adaptive immune system is in an evolutionary arms race against an exponentially-growing pathogen population. That evolutionary pressure selects for efficient detection of, and response to, infection (Hedrick, 2004). Therefore we hypothesise that evolutionary pressure has produced an efficient mechanism for bringing T cells and DCs together, providing a model that can be used for random robotic search.

In this study, we use concepts derived from analysis of T cell search within lymph nodes to inform random robotic search. We identify the type of search used by T cells, then apply the observed three-dimensional search characteristics to a simple continuous space model. We simulate and characterize the performance of T cell inspired search strategies in robots using the iAnt robot system (Hecker et al., 2013). We found heavy-tailed search to be so effective for our simulated iAnts that we have begun incorporating it into the current multi-robot foraging algorithm. We find that T cells use a heavy tailed Lévy search and we show that this search strategy is more efficient than normally distributed random search.

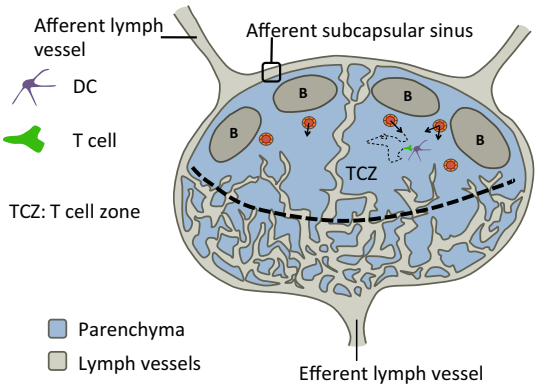

Figure 1: Diagram of a lymph node where T cells search for DCs.

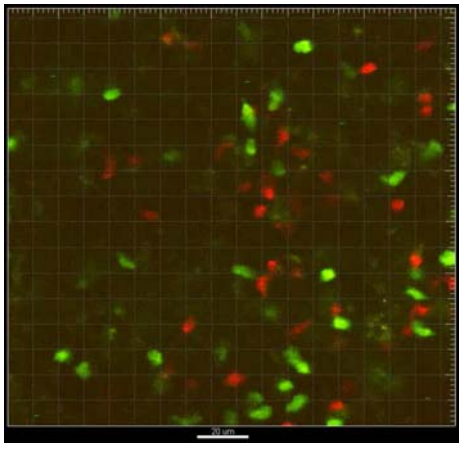

Figure 2: Image frame taken through two-photon microscopy of T cells (red and green) moving in the lymph node. The scale bar at the bottom of the image is 20 µm.

Distribution	Formula	Parameters
Normal	$\frac{e^{-\frac{(x-\mu)^2}{2\sigma^2}}}{\sigma\sqrt{2\pi}}$	$\sigma > 0, \mu > 0$
Exponential	$\frac{1}{\mu}e^{-\frac{x}{\mu}}$	μ
Log-normal	$e^{\frac{e^{-\frac{(x-\mu)^2}{2\sigma^2}}}{\sigma\sqrt{2\pi}}}$	$\sigma > 0, \mu$
Gamma	$\frac{1}{b^a\Gamma(a)}x^{a-1}e^{\frac{-x}{b}}$	a, b
Power-law	$\frac{1}{\sigma}\left(1-k\frac{x-\theta}{\sigma}\right)^{-1-\frac{1}{k}}$	k, σ, θ

Table 1: Definitions and parameters for the five probability density functions used to model random motion.

Stochastic Search

Search in 2- or 3-dimensional space is a common task in biological and engineered systems. Deterministic search strategies may be effective in relatively fixed environments where the distribution of search targets is known *a priori*. However, in environments where target distributions are unknown or change over time randomized search strategies are more effective (Stephens and Krebs, 1986; Acar et al., 2003).

Brownian motion is a common model of random walks. The turning angle between each step is drawn from a uniform distribution (Table 1, row 1).

Viswanathan et al. (2002), among others, described Lévy walks as a model for random walks that differs from classical Brownian motion. In that formulation, step lengths are drawn from a PDF over a power-law distribution. Power-law PDFs are scale-free and have heavy-tails with infinite variance. As a consequence, Lévy walks have many small steps and monotonically decreasing but non-zero probability of taking very large steps (or steps of any finite size). We use the Pareto (1895) formulation of the power law PDF (Table 1, row 5).

We define heavy-tailed distributions to be those with positive tails that approach zero less quickly than the exponentially-distributed PDF (the sub-exponential criteria, Bryson (1974)). Among many others, the log-normal (Table 1, row 3) and power-law distributions meet this criteria, whereas the normal and exponential distributions do not. We follow Shlesinger et al. (1999) in defining the heavy-tailed distribution of velocities (step lengths per time increment) as a *Lévy drive* and reserve Lévy walk for a heavy-tailed distribution of step-lengths with no time component.

Benhamou (2004) argues that Lévy walks are commonly misidentified and that the true picture is often of switching between travel phases from cluster to cluster and Brownian motion once a cluster is found. This pattern of search can be modelled by a correlated random walk (CRW) (Gillis, 1955;

Kareiva and Shigesada, 1983). CRWs are a class of random walks that incorporate non-uniform distributions in turning angle (Mårell et al., 2002).

Related Robotics Work

Simulated robots have used Lévy walks in combination with chemotaxis-inspired gradient sensing (Nurzaman et al., 2009) and artificial potential fields (Sutantyo et al., 2010) to efficiently search unmapped spaces with range-limited sensors. In contrast we consider *free* Lévy drives in this study which do not allow long-range interactions between target and searcher.

In work related to our own, Van Dartel et al. (2004) evolved primitive neural controllers for agents foraging in a simulated world. They observed emergent Lévy walk patterns associated with increasing fitness, converging on parameters consistent with optimal foraging behaviour described by Viswanathan et al. (1999).

Harris et al. (2012) in their supplemental material describe computer simulation of Brownian motion and the generalized Lévy-walk search in a sphere. They report that the Lévy-walk was able to detect targets more efficiently than Brownian motion.

Methods

T Cell Observations

Lymph nodes were prepared according to the protocol described previously by Matheu et al. (2007). T cells were purified by nylon wool according to Allenspach et al. (2001) and labelled with one of two fluorescent dyes: 1 µM (micromolar) Carboxyfluorescein diacetate succinimidyl ester (CFSE) or 5 µM 5-(and-6)- (((4-Chloromethyl) Benzoyl) Amino) Tetramethylrhodamine (CMTMR). 5 to 10×10^6 labelled T cells were injected intravenously into recipient mice. Fifteen to 18 hours later, after T cells migrated into lymph nodes, the inguinal lymph nodes were removed and recorded using two photon-imaging.

Imaging experiments were performed using a Biorad Radiance 2000 scanner mounted on an Olympus upright microscope with a chamber temperature of 37 °C. Explanted lymph nodes were incubated with a 37 °C solution of Dulbecco's Modified Eagle Medium (DMEM) bubbled with 95% O_2 and 5% CO_2 in order to preserve cell motility (Huang et al., 2007). T cell behaviour within a lymph node was monitored in the T cell area at a minimum of 70 µm below the surface of the node. For 4D (3 spatial+1 time) analysis of T cell motility, multiple stacks in the z axis (z step = 3 µm) were acquired every 15-20 s (depending on the number of z stacks acquired) for 15-40 min, with an overall field thickness of 40-60 µm.

Cell motility was analysed with Imaris 6.0 (Bitplane AG, Zurich, Switzerland). Tracks that lasted less than 3 time steps were removed from consideration. Tracks with total length or displacement from the start location less than 17 µm over the course of the observation were assumed to be non-motile and discarded.

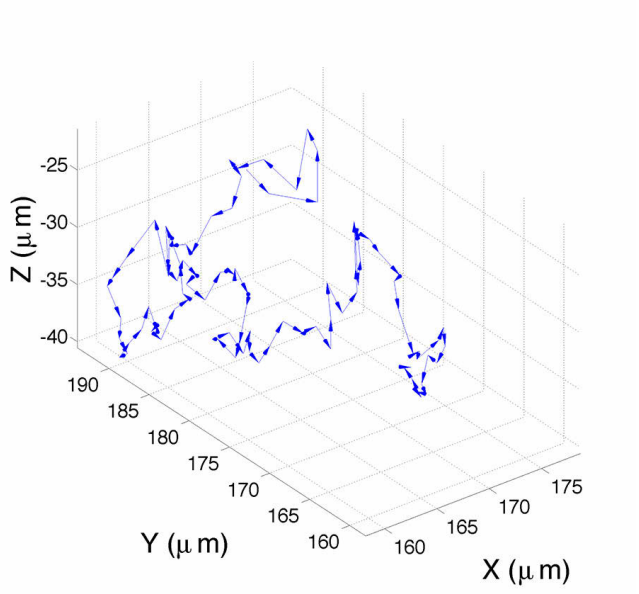

Figure 3: Example T cell track visualized from experiment data. Cell positions were captured every 14.93 seconds.

The point sequences generated by Imaris were used to create position vectors joining adjacent cell locations and the Euclidean norm for each vector was calculated. This provides a distribution of step sizes that were fit to probability distributions using Maximum Likelihood Estimation (MLE) described by Myung (2003).

The lab observations described were replicated seven times, resulting in 63,812 steps in 3,110 T cell tracks. The maximum velocity over all observations is $1.9\,\mu m\,s^{-1}$ with a mean of $0.11\,\mu m\,s^{-1}$.

Characterizing T Cell Search

Observed T cell population step sizes were fit to more than 50 PDFs. Of those distributions 5 PDFs were selected for further analysis: normal, log-normal, exponential, power-law and gamma. Harris et al. (2012) among others used normal and power-law PDFs to describe cell motion. Log-normal and exponential distributions are well known models of many biological processes. These four distributions form null hypotheses about the motion that we might expect to observe. The gamma probability density function is included because we found that, for several of the observations, it was the best model of the observed step-size distribution (Table 1).

In all cases, the bin sizes and binning methods were varied in order to reduce the effect of bin sizes on distribution fits. Adaptive binning rules described by Freedman and Diaconis (1981) were utilized along with various fixed bin sizes. Binning effects were not observed to be a factor in the fits.

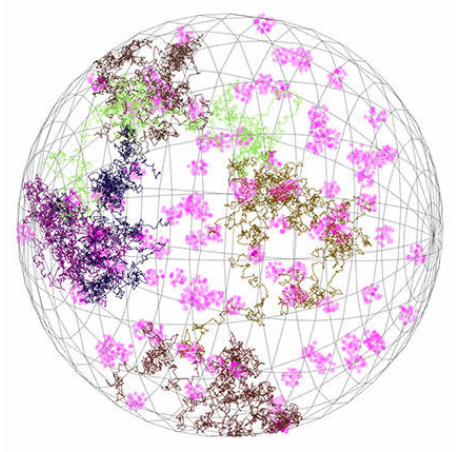

Figure 4: Clusters of targets with searcher tracks. Undiscovered DCs are pink, discovered DCs are red. Each coloured track corresponds to the path followed by each of the 6 searchers. 100 clusters of 30 targets are shown.

The relative *goodness of fit* (GoF) of each PDF to empirical data was evaluated using the Kolmogorov-Smirnov, the Bayesian information criterion (BIC), described in and the Akaike information criterion (AIC), as well as with log-likelihood measures (Table 2). Anderson-Darling calculates the integral of the area between the empirical data and the PDF. The Kolmogorov-Smirnov test matches the mean and variance of the observed data to the PDF and tests for normality. AIC and BIC incorporate the number of parameters available in the PDF to be fit to the observed distribution into the GoF value. AIC and BIC measure the information lost by replacing the observed data with a model.

Controversy exists around the identification of power-law PDFs and associated claims of Lévy walk observation. Many data sets that were not generated by a power-law PDF can be fit to a power-law distribution (Reynolds, 2008). We use techniques developed by Clauset et al. (2009) to address the fitting problems unique to power-law distributions. Distributions were fit to data and goodness of fit calculations were made in MATLAB and Statistics Toolbox Release 2013a (The MathWorks, Inc., Natick, Massachusetts, United States. 2013).

In order to determine whether the distribution of step sizes observed in the total population was due to the distribution of step sizes across tracks or within tracks we used the method of Petrovskii et al. (2011). Each track was scaled by the mean step length of that track and the distribution of the scaled tracks compared to the original tracks. Since the distribution was preserved after tracks were scaled the distribution is due to intra-track step lengths rather than differences in track means.

Simulation in a 3D domain

Our 3D simulation models the search space as a continuous unit sphere (Fig. 4). For these experiments we used $m = 16,384$ targets divided into n clusters, giving a target detection density on the same order as that estimated for DCs in lymph nodes.

Searchers were considered to have discovered a target if they came within a parameterized distance γ of a target. Targets were only available for discovery once. Search steps are treated as discrete in a continuous space, so detection of targets is checked at the end of each step and not at intermediary points. This detection radius encompasses the possible role of chemical gradients and DC dendrites reaching out into the surrounding space. Both mechanisms could be modelled by increasing γ.

Brownian motion is modelled as a sequence of fixed step lengths with uncorrelated turning angles. This results in motion that in the aggregate consists of movements along a trajectory (perhaps containing multiple steps) which is uncorrelated over any sub-sequence of trajectories. This formulation satisfies properties of Brownian motion identified by Einstein (1905): that trajectory lengths are uncorrelated, and displacement from a starting location tends towards a normal distribution. We tested this conclusion by repeating our experiments with Brownian motion modelled by step sizes drawn from a normal distribution and found the same performance.

Paths corresponding to the log-normal, exponential, gamma and power-law distributions were created using the same procedure, except that the scaling radial length was drawn from a PDF in which the mean value μ is equal to r. This allows search to make relatively long jumps while making most of the jumps closer to the fixed step size of the discrete random walk. The simulation was written in C++ and PDFs calculated using the BOOST C++ Libraries 1.53.0 (Austern, 2005).

iAnt Robot System

iAnt robots (Hecker et al., 2012) implement ant-inspired algorithms that mimic colonies of seed-harvester ants using a combination of individual memory and pheromone trail to collect resources and carry them to a central nest. Robots are equipped with ultrasound sensors, compasses, and cameras (Fig. 5) mounted on the robots which enable them to search for and find resources placed in various configurations. The iAnt simulator replicates the movement and sensing capabilities of these robots. iAnt behaviour has several phases, including a random search phase. The parameters for this search are determined by a genetic algorithm (GA) which evolves simulated iAnts and produces a strategy for the physical robots to use in the real resource collection task. Targets were distributed into 32 piles of 32 tags.

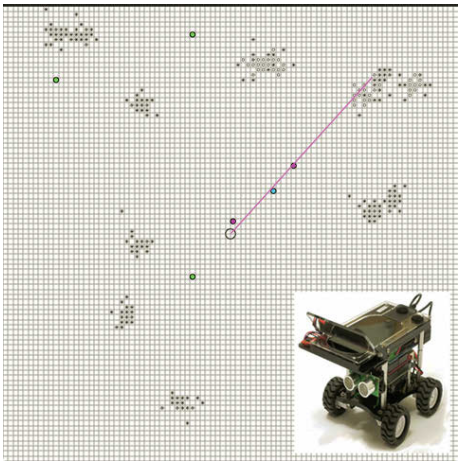

Figure 5: Simulation of the physical iAnt robots. Grey dots are QR tags which are the target of search. Circles are robot locations. Blue circles indicate a robot that has found a tag and is returning to a central location. Green circles are robots engaged in search. The pink line is a pheromone trail. Each of the 6 iAnts we have built is run by an on-board iPhone.

Adaptive correlated random walk (ACRW) In previous implementations, robots explored an experimental area using a random walk with fixed step size and a direction drawn from a normal distribution (Table 1, row 1). The standard deviation σ determines how correlated each step is with the previous step. In the ARCW σ varies depending on the observed density of targets in the search location. The search pattern therefore depends on the local density of targets observed by the robot.

We implemented five search strategies in simulation and compared them to one another: Brownian motion, a Lévy-like (log-normal) strategy, correlated log-normal, and two adaptive correlated random walks. The original ACRW used normally distributed step sizes; we compare that to an adaptive walk with log-normal distributed step sizes. With the exception of Brownian motion, each strategy has different parameters that are evolved by the iAnt genetic algorithm (GA). Log-normal search uses an evolved standard deviation to parameterize its log-normal step length distribution. Correlated log-normal search includes a second evolved standard deviation to parameterize a normal distribution of step angles. The adaptive correlated normal search has two evolved parameters that adapt step angle correlation, depending on whether robots have previously found resources or followed a pheromone trail. Adaptive correlated log-normal search uses the same two parameters to adapt step angle, as well as a third parameter to control the distribution of step lengths.

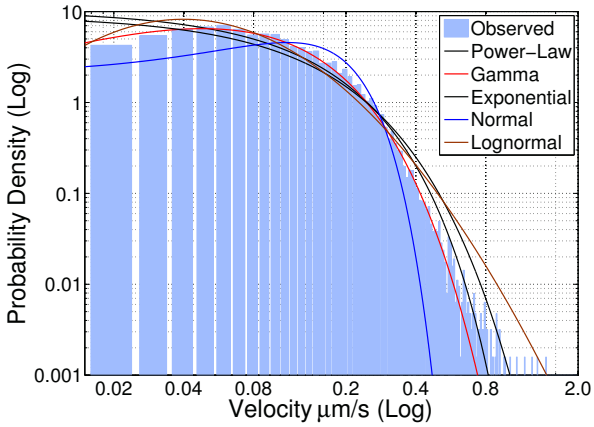

Figure 6: PDFs fit to a probability histogram of T cell velocities taken from all 7 experiments. Qualitatively and quantitatively the log-normal and gamma distributions fit the data more closely than the normal distribution. The normal distribution underpredicts how often large velocities occur, the log-normal distribution slightly underpredicts the number of small values, while the gamma distribution slightly underpredicts the number of large values.

Distribution	AICc ($\times 10^5$)	Log-likelihood ($\times 10^4$)	K-S	Relative AICc
Normal	-1.29	-6.49	$0.12, p = 0$	0.84
Exponential	-1.52	-7.60	$0.1413, p = 0$	0.94
Log-normal	-1.59	-7.95	$0.0748, p = 0$	0.97
Gamma	-1.62	-8.11	$0.0460, p = 0$	0.98
Power-Law	-1.64	-8.23	$0.0888, p = 0$	1.0

Table 2: Goodness of fit using Akaike information criterion with finite size correction (AICc), Kolmogorov-Smirnov (K-S), and Log-likelihood tests.

Results

Characterizing T Cell Search

In all cases BIC and AIC measures were in agreement so only AIC results are presented.

We first asked what type of PDF best describes the type of T cell search occurring in lymph nodes. Table 2 shows the relative goodness of fit for each of the PDFs we considered when applied to the entire data set of T cell velocities. The K-S test rejects all the candidates as acceptable fits (small p-values), this is mostly due to the very large number of data points being fit. As the number of points increases, the tolerance for any deviation from the ideal analytic curve is reduced. Since empirical data necessarily differs from the ideal parametric PDF, with enough data points no distribution will be accepted as a fit to the data (i.e. fail to reject H_0 that the observed data and proposed model come from the same PDF). As a result we use the AICc and log-likelihood methods to evaluate how well the distributions fit our data. Lower values for the three tests indicate better fits.

Considering the seven observational experiments sepa-

Distribution	Parameters
Normal	mean (μ) = 0.11, sigma (σ) = 0.08
Exponential	mean (μ) = 0.1118
Log-normal	log location (μ) = -2.5024, log scale(σ) = 0.84
Gamma	Shape (a) = 1.75 , Scale (b) = 0.06
Power-Law	Shape (k) = -0.05, Scale (σ) = 0.1, Threshold (θ) = 0.01

Table 3: Maximum likelihood parameter estimates.

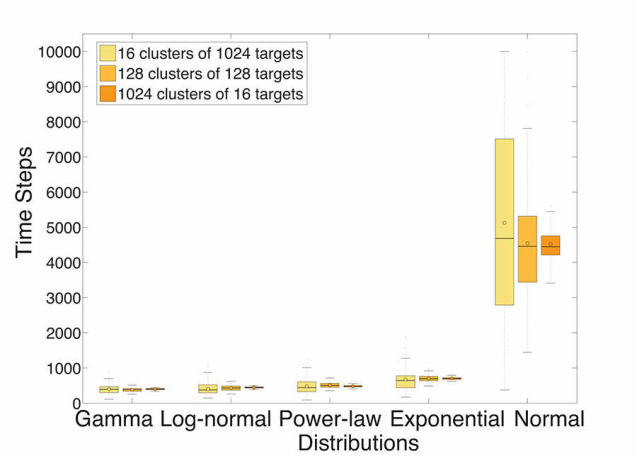

Figure 7: Comparison of search strategy performance across changes in target distribution. The y-axis is time for 6 searchers to find 1,000 targets. Bar = median, circle = mean.

rately resulted in power-law, log-normal and the gamma distributions being the top three fits, with one exception where the normal distribution ranked third in a single experiment. While all distributions are rejected by the Kolmogorov-Schmirnov test when fit to all the data, heavy-tailed distributions fit to individual experiments are not rejected. This leads us to believe that the data are not perfectly represented by any particular distribution, though our analysis shows that the heavy tailed distributions are the best models to describe T cell movement in lymph nodes.

3D Performance

We then modelled search efficiency to test the search performance of heavy tailed distributions and normal distributions using the model shown in Fig. 4. Evaluation of the search performance in simulation reinforces the functional similarity between the two heavy-tailed distributions (log-normal and power-law) and the gamma distribution which was parameterized to take on a heavy-tailed form. The two non-heavy tailed search strategies (exponential and normal) failed to discover targets as quickly as the heavy-tailed search strategies (Fig. 7). Distribution parameters for the simulation were taken from those observed in PDFs fit to T cell motion (Table 3).

Heavy-tailed search did better than its competitors in finding targets quickly and with lower variance. Heavy-tailed search continues to find targets quickly when targets are

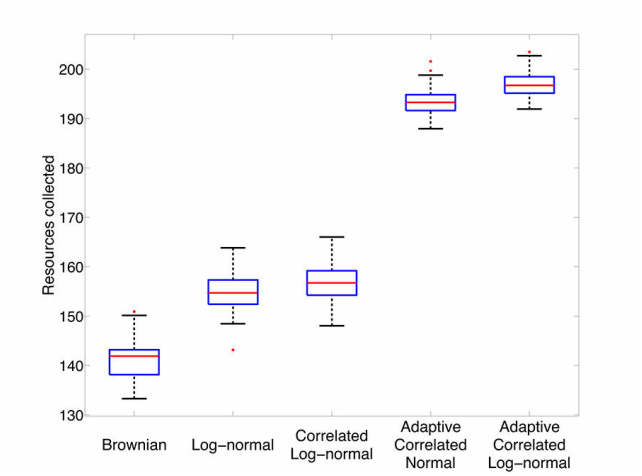

Figure 8: Comparison of search strategies in the iAnt simulator. We compare Brownian search, log-normal search, and adaptive correlated random walk strategies. While the heavy-tailed log-normal search performs better that Brownian search the correlated random walk is able to collect 25% more QR tags, and the adaptive correlated walks are able to collect 42% more tags in the same period.

highly clustered and separated by voids because they are able to cover gaps in less time than Brownian motion can. The cost heavy-tailed distributions pay is that they do not search the area they are in as exhaustively as Brownian motion. If a Brownian searcher happened to start near a cluster of targets it discovered many of those targets. If clusters were further removed from the searcher's initial placement then Brownian motion would have difficulty reaching the nearest cluster in a reasonable amount of time, this results in the high variance seen in Fig. 7. Heavy-tailed search is not as susceptible to the initial distribution because the rare but relatively large step sizes allow distances to be covered quickly so initial conditions to have less impact on search success. Results presented are for 6 searchers but we observed similar behaviour for single searcher experiments.

iAnt Performance

We then applied the heavy tailed step size to the iANT robot simulation system for robotic target search. Performance of Brownian, log-normal, correlated log-normal, adaptive correlated Brownian and adaptive correlated log-normal search is shown in Fig. 8. The log-normal distribution was chosen to represent the heavy-tailed distributions due to simplicity of implementation and easy comparison to the normal distribution of Brownian motion.

The results for the 2D iAnt simulation were consistent with those from the 3D simulation. The heavy-tailed log-normal search outperformed Brownian motion in the iAnts. The adaptive strategies correspond to correlated random walks in which the correlation between step angles de-

pends on the target environment observed by the robots. Both adaptive search strategies significantly outperformed the non-adaptive algorithms. Robots using log-normal adaptive search collected more resources compared to robots using adaptive Brownian search. This difference is small but statistically significant: $n = 198, 9.8\%, p < 0.001$.

The observed Lévy-walk pattern of step-sizes produced by the iAnt simulation performing the adaptive Brownian correlated walk are heavy-tailed.

Discussion

We find that T cell movement in lymph nodes is better characterized by three different heavy-tailed distributions, power-law, log-normal and gamma than by exponential or Brownian motion (Fig. 6). Brownian and exponential distributions have commonly been used to model many processes in biology, economics, and physics (Mitzenmacher, 2004); however more recently, biological movement, including T cell movement through brain tissue (Harris et al., 2012), has been described by Lévy walks. Our results agree with previous studies showing that many biological systems adopt heavy tailed motion strategies, but do not follow an ideal power-law distribution of step sizes.

We have demonstrated that heavy-tailed distributions fit T cell motion in lymph nodes well, and are effective search strategies. Two of those heavy-tailed distributions are the log-normal and power-law distributions; Mitzenmacher (2004) discusses the history of debate across many fields and at many times regarding whether the lognormal or power-law distributions best model various phenomena. The heavy-tailed search strategies we simulated showed similar performance characteristics to one another. In that sense at least the particular distribution does not appear to matter as long as it allows a mixture of long steps with low likelihood and many small steps with high probability.

Our lymph node simulations show that the three heavy-tailed distributions search equally well, and much better than Brownian motion (Fig. 7). This is true of search for DCs distributed in a wide range of cluster densities. Thus the question of whether step size distributions are precisely power-law may not be relevant for determining the efficiency of the search process.

Viswanathan et al. (1999) shows that Lévy walks are optimal search when target clusters are sparse and targets are relatively slow compared to searchers. Numerous papers identified Lévy walks in biological data sets. Recently T cells have been found to perform Lévy walks in mouse brains as a response to parasitic infection (Harris et al. (2012)).

Using the iANT simulation, we found that walks that adapt to detected resources perform much better than simpler non-adaptive walks. Log-normal adaptive search performed only slightly better than Brownian adaptive search. However, we note that the observed distribution of steps sizes in the Brownian ACRW is also heavy-tailed. The combination of step directions that are correlated over time (an intrinsic property of the robots), and adaptation to detected resources (an extrinsic property of the environment) results in an effective adaptive search.

In robots, the heavy tailed distributions caused by walks that adapt to environmental signals are much more effective than parametric heavy-tailed walks that are not adaptive. However adaptive walks may appear to have a heavy-tailed distribution of step lengths. It is currently unknown whether T cells might use the same adaptation strategy to respond to their environment within the lymph node. The lymph node has a complex structure, which includes the fibroblastic reticular cell (FRC) network (Chai et al., 2013). The FRC scaffold appears to serve multiple functions, but T cells have been observed, at times, to move along the FRC (Bajénoff et al., 2006). If the FRC network partially governs the motion of T cells, it would be considered an extrinsic factor as opposed to intrinsic cellular motion. Since T cells, and the lymph node in which they search for DCs, are here considered as part of the same system, we do not distinguish between intracellular and extracellular factors controlling the pattern of search. Therefore, even though extrinsic factors can shape T cell motion in vivo, our study doesn't discriminate whether T cells adapt their walks according to environmental cues in the lymph node. However this work suggests that as a hypothesis worth exploring.

In conclusion, our observations of T cell motion provided inspiration for efficient search in our robot systems and conversely observation of search in those robot systems has provided insight into the possible advantages that search pattern may provide to the immune system.

References

Acar, E. U., Choset, H., Zhang, Y., and Schervish, M. (2003). Path planning for robotic demining: Robust sensor-based coverage of unstructured environments and probabilistic methods. *The International Journal of Robotics Research*, 22(7-8):441–466.

Allenspach, E. J., Cullinan, P., Tong, J., Tang, Q., Tesciuba, A. G., Cannon, J. L., Takahashi, S. M., Morgan, R., Burkhardt, J. K., and Sperling, A. I. (2001). Erm-dependent movement of cd43 defines a novel protein complex distal to the immunological synapse. *Immunity*, 15(5):739–750.

Austern, M. (2005). Proposed draft technical report on c++ library extensions. *N1745*, pages 05–0005.

Bajénoff, M., Egen, J. G., Koo, L. Y., Laugier, J. P., Brau, F., Glaichenhaus, N., and Germain, R. N. (2006). Stromal cell networks regulate lymphocyte entry, migration, and territoriality in lymph nodes. *Immunity*, 25(6):989–1001.

Benhamou, S. (2004). How to reliably estimate the tortuosity of an animal's path:: straightness, sinuosity, or fractal dimension? *Journal of Theoretical Biology*, 229(2):209–220.

Birk, A. and Carpin, S. (2006). Rescue roboticsa crucial milestone on the road to autonomous systems. *Advanced Robotics*, 20(5):595–605.

Bryson, M. C. (1974). Heavy-tailed distributions: properties and tests. *Technometrics*, 16(1):61–68.

Chai, Q., Onder, L., Scandella, E., Gil-Cruz, C., Perez-Shibayama, C., Cupovic, J., Danuser, R., Sparwasser, T., Luther, S. A., Thiel, V., et al. (2013). Maturation of lymph node fibroblastic reticular cells from myofibroblastic precursors is critical for antiviral immunity. *Immunity*.

Clauset, A., Shalizi, C. R., and Newman, M. E. (2009). Power-law distributions in empirical data. *SIAM review*, 51(4):661–703.

Einstein, A. (1905). The theory of the brownian movement. *Ann. der Physik*, 17:549.

Fink, W., Dohm, J. M., Tarbell, M. A., Hare, T. M., and Baker, V. R. (2005). Next-generation robotic planetary reconnaissance missions: a paradigm shift. *Planetary and Space Science*, 53(14):1419–1426.

Freedman, D. and Diaconis, P. (1981). On the histogram as a density estimator: L 2 theory. *Probability theory and related fields*, 57(4):453–476.

Gillis, J. (1955). Correlated random walk. In *Mathematical Proceedings of the Cambridge Philosophical Society*, volume 51, pages 639–651. Cambridge Univ Press.

Harris, T. H., Banigan, E. J., Christian, D. A., Konradt, C., Wojno, E. D. T., Norose, K., Wilson, E. H., John, B., Weninger, W., Luster, A. D., et al. (2012). Generalized lévy walks and the role of chemokines in migration of effector cd8+ t cells. *Nature*, 486(7404):545–548.

Hecker, J. P., Letendre, K., Stolleis, K., Washington, D., and Moses, M. E. (2012). Formica ex machina: ant swarm foraging from physical to virtual and back again. In *Swarm Intelligence*, pages 252–259. Springer.

Hecker, J. P., Stolleis, K., Swenson, B., Letendre, K., and Moses, M. E. (2013). Evolving Error Tolerance in Biologically-Inspired iAnt Robots. In *ECAL 2013 (in press)*.

Hedrick, S. M. (2004). The acquired immune system-a vantage from beneath. *Immunity*, 21(5):607–616.

Hu, H., Oyekan, J., and Gu, D. (2011). A school of robotic fish for pollution detection in port. *Biologically Inspired Robotics (Y. Liu and D. Sun, eds.)*, pages 85–104.

Huang, J. H., Cárdenas-Navia, L. I., Caldwell, C. C., Plumb, T. J., Radu, C. G., Rocha, P. N., Wilder, T., Bromberg, J. S., Cronstein, B. N., Sitkovsky, M., et al. (2007). Requirements for t lymphocyte migration in explanted lymph nodes. *The Journal of Immunology*, 178(12):7747–7755.

Kareiva, P. and Shigesada, N. (1983). Analyzing insect movement as a correlated random walk. *Oecologia*, 56(2-3):234–238.

Mackay, I. R., Rosen, F. S., von Andrian, U. H., and Mackay, C. R. (2000). T-cell function and migrationtwo sides of the same coin. *New England Journal of Medicine*, 343(14):1020–1034.

Mårell, A., Ball, J. P., and Hofgaard, A. (2002). Foraging and movement paths of female reindeer: insights from fractal analysis, correlated random walks, and lévy flights. *Canadian Journal of Zoology*, 80(5):854–865.

Matheu, M. P., Parker, I., and Cahalan, M. D. (2007). Dissection and 2-photon imaging of peripheral lymph nodes in mice. *Journal of Visualized Experiments: JoVE*, (7).

Mirsky, H. P., Miller, M. J., Linderman, J. J., and Kirschner, D. E. (2011). Systems biology approaches for understanding cellular mechanisms of immunity in lymph nodes during infection. *Journal of theoretical biology*, 287:160–170.

Mitzenmacher, M. (2004). A brief history of generative models for power law and lognormal distributions. *Internet mathematics*, 1(2):226–251.

Myung, I. J. (2003). Tutorial on maximum likelihood estimation. *Journal of Mathematical Psychology*, 47(1):90–100.

Nurzaman, S. G., Matsumoto, Y., Nakamura, Y., Koizumi, S., and Ishiguro, H. (2009). Yuragi-based adaptive searching behavior in mobile robot: From bacterial chemotaxis to lévy walk. In *Robotics and Biomimetics, 2008. ROBIO 2008. IEEE International Conference on*, pages 806–811. IEEE.

Pareto, V. (1895). La legge della domanda. *Giornale degli economisti*, 10:59–68.

Petrovskii, S., Mashanova, A., and Jansen, V. A. (2011). Variation in individual walking behavior creates the impression of a lévy flight. *Proceedings of the National Academy of Sciences*, 108(21):8704–8707.

Reynolds, A. (2008). How many animals really do the lévy walk? comment. *Ecology*, pages 2347–2351.

Shlesinger, M. F., Klafter, J., and Zumofen, G. (1999). Above, below and beyond brownian motion. *American Journal of Physics*, 67:1253.

Stephens, D. W. and Krebs, J. R. (1986). *Foraging theory*. Princeton University Press.

Sutantyo, D. K., Kernbach, S., Levi, P., and Nepomnyashchikh, V. A. (2010). Multi-robot searching algorithm using lévy flight and artificial potential field. In *Safety Security and Rescue Robotics (SSRR), 2010 IEEE International Workshop on*, pages 1–6. IEEE.

Van Dartel, M., Postma, E., van den Herik, J., and de Croon, G. (2004). Macroscopic analysis of robot foraging behaviour. *Connection Science*, 16(3):169–181.

Viswanathan, G., Bartumeus, F., V Buldyrev, S., Catalan, J., Fulco, U., Havlin, S., Da Luz, M., Lyra, M., Raposo, E., and Eugene Stanley, H. (2002). Levy flight random searches in biological phenomena. *Physica A: Statistical Mechanics and Its Applications*, 314(1):208–213.

Viswanathan, G., Buldyrev, S., Havlin, S., Da Luz, M., Raposo, E., and Stanley, H. (1999). Optimizing the success of random searches. *Nature*, 401(6756):911–914.

Weber, T. R. (1995). An analysis of lemmings: A swarming approach to mine countermeasures in the vsw/sz/bz. Technical report, DTIC Document.